Ecological speciation of Japanese Hedgehog mushroom: Hydnum subalpinum sp. nov. is distinguished from its sister species H. repando-orientale by means of integrative taxonomy

Ryo Sugawara (ryo.book.12@gmail.com)
Tottori Daigaku https://orcid.org/0000-0002-4233-2076
Wataru Aoki
Shinshu Daigaku
Akiyoshi Yamada
Shinshu Daigaku
Akira Nakagiri
Tottori Daigaku
Naoki Endo
Tottori Daigaku

Research Article

Keywords: Cantharellales, ectomycorrhizal fungi, morphological description, hybrid incompatibility, species delimitation, 1 new taxon

Posted Date: August 9th, 2022

DOI: https://doi.org/10.21203/rs.3.rs-1908123/v1

Abstract

Hydnum repando-orientale is an East Asian species closely related to *H. boreorepandum* and *H. repandum*; all three species produce edible mushrooms. We identified two ecological groups of *H. repando-orientale* in Japan: a temperate group occurring in Fagaceae-dominated forest at < 1200 m a.s.l. (ROF), and a subalpine group occurring in coniferous forest in highland at > 1900 m a.s.l. (ROC). We re-examined the taxonomy of the two ecological groups of *H. repando-orientale* using integrative approaches. Phylogenies of the two ecological groups and other related species were inferred from the internal transcribed spacer (ITS) and gene portions encoding the large subunit of nc rRNA (LSU), translation elongation factor-1 alpha (*TEF1*), RNA polymerase II largest subunit (*RPB1*), and RNA polymerase II second-largest subunit (*RPB2*). The concatenated phylogenetic tree separated the two ecological groups into well-supported sister clades. Also, species delimitations based on the topological congruence (GCPSR) and multispecies coalescent model (GMYC and BP&P) supported to separate the two ecological groups. Morphological analysis showed that ROC specimens had significantly larger basidiospores, compared with ROF specimens. Mon-mon mating tests using six ROF, three ROC, and three *H. boreorepandum* strains each showed independent incompatible groups, whereas one ROC strain showed compatibility with both ROC and ROF populations. Based on these results, we defined the ROC group as a new species, *H. subalpinum*. Because *H. repando-orientale* and *H. subalpinum* have smaller genetic divergence in nc rDNA and maintain slight sexual compatibility, they may have recently speciated in East Asia.

1. Introduction

Hydnum repandum L., the type species of the genus *Hydnum* L., is an ectomycorrhizal fungus. Its morphology characters include large and fleshy basidiomata with cream to orange ochraceous pileus-surface, spinaceous hymenophores, and robust stipe attaching decurrent spines; thin-walled, smooth, hyaline, medium-sized (7.0–8.5 × 6.2–7.5 µm), and subglobose to elongated subglobose basidiospores, produced on four-spored basidia; and monomitic hyphal system composed of clamped, oil-rich hyphae (Niskanen et al. 2018). This species was originally described from Sweden (Linnaeus 1753) but had long been considered a cosmopolitan species in the Northern Hemisphere (Rea 1922; Coker and Beers 1951; Hall and Stanz 1971; Maas Geesteranus 1971; Harrison and Grund 1987); it also had been regarded as an economically important edible mushroom with many vernacular names worldwide, including *"Hedgehog-mushroom," "Sweet-tooth-mushroom," "Pied-de-mouton,"* and *"Kanoshita"* (Kawamura 1913; Phillips 2005; Roberts and Evans 2011). However, recent molecular systematics analyses have suggested that true *H. repandum* is found only in Europe (Grebenc et al. 2009; Olariaga et al. 2012; Yanaga et al. 2015; Feng et al. 2016; Niskanen et al. 2018; Swenie et al. 2018; Sugawara et al. 2022a). In the infrageneric system established by Niskanen et al., *H. repandum* is regarded as the type species of the subgenus *Hydnum* L., which is composed of *H. boreorepandum* Niskanen, Liimat. & Niemelä; *H. olympicum* Niskanen, Liimat. & Ammirati; *H. repando-orientale* Liimat. & Niskanen; *H. repandum*; *H. slovenicum* Liimat. & Niskanen; *H. sphaericum* T. Cao & H. S. Yuan; *H. subolympicum* Liimat. & Niskanen; *H. vagabundum* Swenie, Ovrebo & Matheny; and *H. washingtonianum* Ellis & Everh. (= *H. neorepandum* Niskanen & Liimat.; Swenie et al. 2018) (Niskanen et al. 2018; Swenie et al. 2018; Cao et al. 2021b). The subg. *Hydnum* was further separated into two sections (i.e., *Hydnum* L. and *Olympica* Niskanen, Liimat. & Ammirati) on the basis of phylogeny (Niskanen et al. 2018). Because most species of the subg. *Hydnum* produce similar basidiomata, recent studies have strongly recommended molecular approaches for accurate species identification (Niskanen et al. 2018; Sugawara et al. 2022a).

Hydnum repandum has been also reported from Japan (Kawamura 1913, 1929, 1954; Yasuda 1913; Asahina 1939; Ito 1955; Imazeki and Hongo 1957; Kikuhara 1987; Yanaga 2015; Yanaga et al. 2015; Sugawara et al. 2019). However, most of them were re-identified as *H. alboluteum* R. Sugaw. & N. Endo; *H. albopallidum* R. Sugaw. & N. Endo; *H. cremeoalbum* Liimat. & Niskanen; and *H. repando-orientale* (Yanaga 2015; Yanaga et al. 2015; Niskanen et al. 2018; Sugawara et al. 2022a)—of these, only *H. repando-orientale* has not been re-classified into another subgenus. Currently, only two species of subg. *Hydnum* (i.e., *H. boreorepandum* and *H. repando-orientale*) have been proven to be distributed in Japan (Niskanen et al. 2018; Sugawara et al. 2022a). *Hydnum boreorepandum* and *H. repando-orientale* were recognized as sister species of *H. repandum* in the phylogeny inferred from the nc rDNA internal transcribed spacer (ITS) sequences (Niskanen et al. 2018); these three species were distinguished by their geographical distribution patterns in Eurasia and by forest habitats. *Hydnum repandum* occurs in Europe, *H. repando-orientale* occurs in East Asia, and *H. boreorepandum* occurs in both areas; *H. boreorepandum* prefers coniferous forests in boreal climate, whereas *H. repandum* has a wider range of hosts and climate regions (Niskanen et al. 2018). We discovered two ecological groups of *H. repando-orientale* in Japan: a temperate group (ROF) which occurs in temperate Fagaceae-dominated forests at ≤ 1200 m a.s.l., and a subalpine group (ROC) which occurs in subalpine coniferous-dominated forests at ≥ 2000 m a.s.l. (Sugawara et al. 2022a). A previous study suggested small differences between ROC and ROF groups in terms of morphological characters (basidiospore size) and sequence data [ITS of nc rDNA operon and translation elongation factor 1-alpha (*TEF1*)]. Because we have not found intermediate types in Japan, the two groups may have adapted to their different ecological niches. We tentatively concluded that the ROF and ROC groups are conspecific (= *H. repando-orientale* s. lat.) because of very small variations in ITS sequences between them (< 0.3%); these variations are within the range of common intraspecific variations in the genus *Hydnum* (i.e., 1–1.5% for species delimitation) (Niskanen et al. 2018). However, mating incompatibility among ROF and ROC groups could not be assessed because of the slow growth of their monospore-isolates; thus, the taxonomic designations of the two ecological groups of *H. repando-orientale* require further investigation.

The *Hydnum* species classification emphasizes on the phylogenetic relationships inferred from ITS sequences (Niskanen et al. 2018; Swenie et al. 2018; Cao et al. 2021b; Sugawara et al. 2022a); however, a phylogeny of the non-coding ITS region alone sometimes leads to unreliable data because it depends on the evolutionary history of a single DNA sequence, rather than a species. For this reason, the use of multiple molecular markers is strongly recommended in a taxonomic framework (Lücking et al. 2020; Aime et al. 2021; Cao et al. 2021a). Molecular data from multiple loci contribute to species delimitations based on topological congruence and the multispecies coalescent model. The genealogical concordance phylogenetic species recognition (GCPSR) approach proposed by Taylor et al. (2000) is used in *Fungi* to define phylogenetic species based on congruent clades from multiple genealogies. Coalescent-based species delimitation using multiple loci is a powerful method for estimating evolutionary lineages that involve ancestral polymorphism, which lacks reciprocal monophyly among alleles (Fujita et al. 2012). Unfortunately, species delimitation approaches have not been used in the current classification systems in the genus *Hydnum*. However, these approaches enable the recognition of cryptic (or pseudocryptic) species as part of an integrative taxonomy, together with other species concepts such as morphology, ecophysiology, and hybrid incompatibility (Fujita et al. 2012; Looney et al. 2020; Cao et al. 2021a).

Here, we aimed to (1) reconsider species boundaries among *H. repando-orientale* and related species in Japan by integrative taxonomic approaches, and (2) present a taxonomic treatment for the ROC group of *H. repando-orientale* s. lat. under the nomenclature. Multi-locus molecular phylogeny was inferred from the sequences of the ITS and the large subunit (LSU) of nc rDNA, *TEF1*, RNA polymerase II largest subunit (*RPB1*), and RNA polymerase II second-largest subunit (*RPB2*). In addition, species delimitations were performed using the GCPSR approach and a multispecies coalescent model based on the generalized mixed Yule coalescent (GMYC) and Bayesian framework (BP&P). A mating test using monospore isolates was performed to evaluate mating compatibility among the ROF and ROC groups, as well as *H. boreorepandum*, a sister species of *H. repando-orientale* s. lat. Finally, we performed morphological characterization of basidiomata including a statistical analysis of mean basidiospore size. Based on findings indicating that the ROC and ROF groups are distinct species, we provide a detailed description of the ROC group as a new species.

2. Materials And Methods

2.1. Basidiomata specimens

We examined 33 basidiomata specimens of *H. boreorepandum* and *H. repando-orientale* s. lat. (Table 1): 23 were collected in our studies in 2016–2020 (Sugawara et al. 2019, 2022a); 4 were collected in this study; 2, including holotype of *H. repando-orientale* (TUMH 60745), were loaned from the Tottori University Mycological Herbarium (TUMH), Fungus/Mushroom Resource and Research Center, Faculty of Agriculture, Tottori University; 4 were loaned from the TNS herbarium of the National Museum of Nature and Sciences, Tokyo. These specimens were collected at 25 sites in Honshu, mainland Japan, at 10 to 2500 m a.s.l. (Fig. 1). We defined *H. repando-orientale* s. lat. as the two ecological groups (ROC and ROF) based on the recorded altitude and forest habitat. (Table 1).

2.2. Morphological analysis

The morphological characterization was conducted in accordance with the method in our previous report (Sugawara et al. 2022a). Thirty basidiospores were measured from each of 21 specimens, and previous measurement were reused for 19 specimens. Because the ROC group showed slightly larger basidiospores, compared with the ROF group, we statistically analyzed the mean basidiospore sizes (MBS) by unpaired two-sample Wilcox tests. We also included eight MBS values of *H. repandum* and *H. boreorepandum* measured by Grebenc et al. (2009), Olariaga et al. (2012), and Niskanen et al. (2018); overall, our analysis included measurements of 5 *H. boreorepandum*, 7 *H. repandum*, 11 ROCs, and 16 ROFs. Using the “stats” package in R v.4.0.5 (R Core Team 2021), the length (L) and width (W) of MBS were compared among ecological/phylogenetic groups (ROC, ROF, *H. boreorepandum*, and *H. repandum*) by the function “pairwise.wilcox.test” and the Bonferroni method.

2.3. Monospore isolation

Fresh basidiomata materials were used for monospore isolation, in accordance with the method proposed by Sugawara et al. (2019). Basidiospores from each hymenophore were collected on an axenic plastic Petri dish, suspended in sterile distilled water, and inoculated onto modified Norkrans’ C medium (MNC; Yamada and Katsuya 1995) solidified with 1.5% gellan-gum (MNC1.5G; Sugawara et al. 2019). Using a platinum loop, inoculated spores were streaked in zigzag to create a spore concentration gradient; they were then incubated at 15°C in the dark (MIR-254-PJ, Panasonic Healthcare, Tokyo, Japan). Infrequent (ca. < 1%) basidiospore germination was observed 1–2 months after incubation. When mycelial colonies reached approximately 2 mm diam, each was transferred to MNC medium solidified with 1.5% agar (MNC1.5A). To conduct mating tests, we selected monospore isolates that exhibited better growth and lacked clamp connections on hyphal septa. In total, three strains from three ROC basidiomata, six strains from four ROF basidiomata, and three strains from three *H. boreorepandum* basidiomata were isolated and established from September 2020 Sep to March 2021. The cultures were deposited in the Fungus/Mushroom Resource and Research Center as Tottori University Fungal Culture Collection (TUFC) strains.

2.4. Mating tests

We used only newly obtained strains for mating tests. Monokaryotic strains of the ROC group showed poor growth on MNC1.5A medium (e.g., 0.5 cm diam per 1-month incubation at 20°C); for this reason, we conducted mating tests three times on different dates and under different culture conditions. The first test involved nine monokaryotic strains that showed better growth on MNC1.5A medium from April 27 to August 4, 2021. Mycelial agar blocks (ca. 3 × 3 mm) pre-cultured for 1–2 months at 15°C were cut and placed near a pair-strain for 3-mm spacing on MNC1.5A medium. Next, each mating pair was incubated at 15°C for 2 months, then at 20°C for 2 months. For the second and third mating tests, each mycelium was pre-cultured in MNC liquid medium for 6 weeks and subsequently transferred to MNC medium plates. From this pre-culture, we could obtain enough mycelial biomass from all monokaryotic strains. Then, second and third tests were conducted using MNC1.5A and one tenth concentration of MNC medium solidified with 2.0% agar (1/10MNC2.0A), respectively. Each test was started at 6 Aug 2021 or 12 Aug 2021 and incubated for 2 months at 20°C.

The formation of clamp connections was observed under a light microscope at 200× magnification with a long working-distance objective lens and at 1000× magnification on slide glasses mounted with distilled water. Some strains showed possible crossing between ecological/phylogenetic groups and resulted in intermediate mating incompatibility groups; therefore, we also examined the nuclear phases of hyphae that formed clamp-like cells to determine whether dikaryotization occurs. A portion of mycelium was mounted in a mixture of 4′,6-diamidino-2-phenylindole (DAPI; Fujifilm Wako Pure Chemical, Japan, Osaka) 0.04% (v/v) and Calcofluor White (Fujifilm Wako Pure Chemical) 0.02% (v/v), then observed under a fluorescence microscope (Eclipse Ei, Nikon Imaging, Japan, Tokyo) equipped with a mercury lamp (Intenslight C-HGFI, Nikon Imaging). To assess the viability of descendant mycelium in artificial medium, a clamped mycelium was was inoculated onto a MNC1.5A plate and incubated at 20°C.

2.5. DNA extraction, polymerase chain reaction (PCR) amplification, and sequencing

DNA extraction, PCR amplification, and sequencing analysis were performed as described by Sugawara et al. (2022a). ITS and LSU amplicons were obtained using universal primers for basidiomycetes: ITS1F/ LBW (Gardes and Bruns 1993; Tedersoo et al. 2008) and CTB6/ LR5F (Garbelotto et al. 1997; Tedersoo et al. 2008). *TEF1* and *RPB1* amplicons were obtained using primers for *Hydnum* species [*RPB1*: Hrpb1F or Hrpb1-4F/ Hrpb1-2R or Hrpb1R (Feng et al. 2016)] [*TEF1*: HydTEF1-F/ HydTEF1-R (Sugawara et al. 2022a)]. For PCR amplification of *RPB2*, we first amplified and sequenced several *Hydnum* and ectomycorrhizal *Sistotrema* using universal primers [fRPB2-5F or bRPB2-6F/ RPB2-b7R2 or RPB2-b7.1R (Kretzer and Bruns 1999; Liu et al. 1999)], then designed new primers based on the obtained sequences: HRPB2-5.5F (forward: 5′-GNAAYTGGGGBGACCAGAAG-3′), HRPB2-5.6F (forward: 5′-AAGGCWGGYGTRTCCCAGGT-3′), HRPB2-6.8R (reverse: 5′-GGRTGRATCTCRCAATGTGTCCA-3′), HRPB2-6.9R (reverse: 5′-GRTGRATCTCRCAATGTGTCCA-3′). These primers enabled the amplification of all known Japanese *Hydnum* species (data not shown). The PCR protocol are shown in **Table S1**. The PCR products were directly sequenced with the same or nested primers; bidirectional sequences were assembled using ClustalW (Thompson et al. 1994). We attempted DNA extraction and PCR amplification of protein-coding genes from the holotype specimen of *H. repando-orientale* (TUMH 60745), but we could not successfully extract DNA using the cetyltrimethylammonium bromide (CTAB) method (Gardes and Bruns 1993) or the E.Z.N.A. HP Fungal DNA Kit (Omega Bio-Tek, Norcross, GA, USA). We obtained 113 sequences and deposited them in the International Nucleotide Sequence Database (INSD) under the accession numbers in Tables 2 **and S2**.

Table 2
Sequence data used in the concatenated phylogeny.

Genus/ subgenus	Species	Herbarium/ Personal nos.	Locality	Accession nos.				
				ITS	LSU	*TEF1*	*RPB1*	*RPB2*
Hydnum subg. *Alba*	*H. albomagnum*	AFTOL-ID-471	USA	DQ218305	AY700199	DQ234568	–	DQ234553
	H. cremeoalbum	TUMH 64024	Japan	LC621823	**LC717912**	LC622458	**LC717839**	**LC717872**
subg. *Hydnum*	*H.* aff. *sphaericum*	HKAS78334	China	KU612589	–	KU612768	KU612733	–
	H. boreorepandum	TUMH 64005	Japan	LC621814	**LC717880**	LC622449	**LC717806**	**LC717840**
		TUMH 64006	Japan	LC621815	**LC717881**	LC622450	**LC717807**	**LC717841**
		TUMH 64007	Japan	LC621816	**LC717882**	**LC717873**	**LC717808**	**LC717842**
		TUMH 64008	Japan	LC621817	**LC717883**	LC622451	**LC717809**	**LC717843**
	H. repandum	03129A	Slovenia	KU612574	KU612655	KU612770	KU612732	–
		HKAS93253	Germany	KU612581	–	KU612769	KU612731	–
	H. sphaericum	Wei 10243	China	MW980563	MW979549	–	MW999470	MW999444
	H. subolympicum	F1188765	USA	KU612599	KU612653	–	KU612741	–
	Hydnum sp. 2	HKAS55410	China	KU612596	KU612654	KU612771	KU612729	–
		HKAS82558	China	KU612595	–	KU612772	KU612730	–
	ROC (H. subalpinum)	TUMH 64011	Japan	LC621867	**LC717886**	LC622493	**LC717812**	**LC717846**
		TUMH 64012	Japan	LC621868	**LC717887**	LC622494	**LC717813**	**LC717847**
		TUMH 64013	Japan	**LC717913**	**LC717888**	**LC717874**	**LC717814**	**LC717848**
		TUMH 64014	Japan	LC621869	**LC717889**	LC622495	**LC717815**	**LC717849**
		TUMH 64015	Japan	LC621870	**LC717890**	LC622496	**LC717816**	**LC717850**
		TUMH 64016	Japan	LC621871	**LC717891**	LC622497	**LC717817**	**LC717851**
		TUMH 64017	Japan	LC621872	**LC717892**	LC622498	**LC717818**	**LC717852**
		TUMH 64629	Japan	**LC717914**	**LC717893**	**LC717875**	**LC717819**	**LC717853**
		TUMH 64630	Japan	**LC717915**	**LC717894**	**LC717876**	**LC717820**	**LC717854**
		TNS-F-80714	Japan	LC621865	**LC717884**	LC622488	**LC717810**	**LC717844**
		TNS-F-85326	Japan	LC621866	**LC717885**	LC622489	**LC717811**	**LC717845**
	ROF (*H. repando-orientale*)	TUMH 62860	Japan	LC377883	**LC717900**	LC622490	**LC717826**	**LC717860**
		TUMH 63125	Japan	LC377886	**LC717901**	LC622491	**LC717827**	**LC717861**
		TUMH 63126	Japan	LC377887	**LC717902**	LC622492	**LC717828**	**LC717862**
		TUMH 64069	Japan	LC621873	**LC717903**	LC622499	**LC717829**	**LC717863**
		TUMH 64071	Japan	LC621875	**LC717896**	LC622500	**LC717822**	**LC717856**
		TUMH 64072	Japan	LC621876	**LC717897**	LC622501	**LC717823**	**LC717857**
		TUMH 64073	Japan	LC621877	**LC717898**	LC622502	**LC717824**	**LC717858**
		TUMH 64074	Japan	LC621878	**LC717899**	LC622503	**LC717825**	**LC717859**
		TNS-F-78326	Japan	LC621864	**LC717895**	LC622487	**LC717821**	**LC717855**

Bold, newly obtained sequences. –, sequence not available.

Genus/ subgenus	Species	Herbarium/ Personal nos.	Locality	Accession nos.				
				ITS	LSU	*TEF1*	*RPB1*	*RPB2*
subg. *Pallida*	*H. albopallidum*	TUMH 63997	Japan	LC621807	**LC717904**	LC622442	**LC717830**	**LC717864**
	H. pallidomarginatum	Yuan 13928a	China	MW980566	MW979552	–	MW999473	MW999447
subg. *Rufescentia*	*H. mulsicolor*	TUMH 63094	Japan	LC377892	**LC717911**	LC622472	**LC717838**	**LC717871**
	H. itachiharitake	TUMH 64032	Japan	LC621829	**LC717905**	LC622461	**LC717831**	**LC717865**
	H. jussii	Yuan 14008	China	MW980553	MW979539	–	–	MW999436
	H. longibasidium	Wei 10383	China	MW980556	MW979541	–	MW999464	MW999438
	H. pallidocroceum	Yuan 14023	China	MW980568	MW979554	–	–	MW999449
	H. umbilicatum	TUMH 63128	Japan	LC377891	**LC717909**	LC622516	**LC717836**	**LC717869**
	H. ventricosum	Yuan 14536	China	MW980561	MW979547	–	MW999468	MW999442
Subgenus Incertae sedis	*H. flavidocanum*	Yuan 13903a	China	MW980559	MW979545	–	MW999466	MW999441
	H. minus	TUMH 64050	Japan	LC621842	**LC717910**	LC622470	**LC717837**	**LC717870**
	H. orientalbidum	TUMH 62998	Japan	LC377875	**LC717908**	LC622478	**LC717835**	**LC717868**
	H. tomaense	TUMH 64086	Japan	LC621885	**LC717907**	LC622509	**LC717834**	**LC717867**
Sistotrema	*S.* aff. *albopallescens*	TUMH 62071	Japan	LC621901	LC667373	LC622522	–	LC667370
	S. aff. *muscicola*	TUMH 63116	Japan	LC621902	LC667374	LC622523	**LC717833**	LC667372
	S. aff. *confluens*	SuR20201011-303	Japan	**LC717916**	**LC717906**	**LC717877**	**LC717832**	**LC717866**
	S. chloroporum	TUMH 64409	Japan	LC642034	LC642057	**LC717878**	–	LC667369
	S. flavorhizomorphae	TUMH 64399	Japan	LC642049	LC642067	**LC717879**	–	LC667371

Bold, newly obtained sequences. –, sequence not available.

2.6. Phylogenetic analyses

Phylogenetic analyses were performed based on the (i) ITS dataset and (ii) concatenated dataset of five loci (ITS, LSU, *TEF1*, *RPB1*, and *RPB2*). The ITS dataset included sequences of Holarctic species of the genus *Hydnum* downloaded from the INSD/UNITE databases, which comprised > 60 phylogenetic species (**Table S2**; Olariaga et al. 2012; Yanaga et al. 2015; Niskanen et al. 2018; Swenie et al. 2018; Cao et al. 2021b; Sugawara et al. 2022a). As an outgroup, we selected mycorrhizal *Sistotrema* spp. (Yanaga et al. 2015; Niskanen et al. 2018; Sugawara et al. 2022a); we excluded *S. confluens* Pers. and *S. subconfluens* L.W. Zhou because they showed extremely high genetic divergence in the ITS sequences (Niskanen et al. 2018; Sugawara et al. 2022b). The 175 ITS sequences including the outgroup were sampled and automatically aligned using MAFFT online v. 7 (Katoh et al. 2019). The alignment was manually refined, and the best substitution model for RAxML program was estimated using ModelTest-NG v. 0.2.0 (Flouri et al. 2015; Darriba et al. 2020). We identified the best maximum likelihood tree using the rapid bootstrap algorithm in RAxML v. 8.2.10 (Stamatakis 2014) on the raxmlGUI v. 2.0.5 platform (Edler et al. 2021). This analysis was computed under a HKYGAMMA substitution model with 1,000 replications of bootstrap analyses (MLBS).

A more detailed phylogenetic analysis was performed using the sequences of five loci (ITS, LSU, *TEF1*, *RPB1*, and *RPB2*) obtained from 24 materials of *H. boreorepandum*, the ROC group, and the ROF group. Other taxa belonging to the subg. *Hydnum* were included in the dataset if ≥ 3 sequences of the five loci to be analyzed were available in the INSD. Furthermore, 20 taxa of *Hydnum* and *Sistotrema* spp. were used as outgroups, among which 45 sequences were newly obtained (Table 2) in this study. Thus, 51 total taxa was included in the second analyses.

First, we annotated each locus and constructed independent phylogenies. The ITS and LSU sequences were contiguously connected and subsequently annotated using ITSx v. 1.1.3 (Bengtsson-Palme et al. 2013) on the PlutoF workbench (Abarenkov et al. 2010). The portions of protein coding genes (*TEF1*, *RPB1*, and *RPB2*) were independently aligned and annotated based on the following references: DQ234568 (*H.*

albomagnum) for *TEF1* (Matheny et al. 2007), EF014376 and KU612731 (*H. repandum*) for *RPB1* (Liu et al. 2006; Feng et al. 2016), and DQ234553 (*H. albomagnum*) for *RPB2* (Matheny et al. 2007). *TEF1* includes three coding (ca. 500 bp) and two intronic regions (ca. 100 bp); *RPB1* comprises mostly a coding region (ca. 850 bp) with a small intronic region (ca. 15 bp); *RPB2* has only a coding region (ca. 800 bp). The RAxML phylogenies were independently constructed using each alignment as described above. The following substitution models were selected as recommended by ModelTest-NG: GTRGAMMAI for ITS + LSU, HKYGAMMAI for *TEF1*, GTRGAMMAI for *RPB1*, and GTRGAMMA for *RPB2*. For phylogenetic analysis of the concatenated dataset using MrBayes v. 3.2.7 (Ronquist et al. 2012), we determined the partitioning schemes and substitution models using PartitionFinder 2 v. 1.1 (Lanfear et al. 2017) under a "greedy" scheme search algorithm (Lanfear et al. 2012) and AICc criteria. By this analysis, we set nine subsets that included independent substitution models as shown in Table 3. Because the *TEF1* alignment showed partition scheme trends that differed from the *RPB1* and *RPB2* alignments, we performed further model estimation and scheme search. Next, PartitionFinder 2 analysis was performed on only the *TEF1* alignment under an "all" scheme search algorithm, in which all possible combinations of data blocks were analyzed. This analysis yielded the same partitioning scheme as greedy option; thus, we adopted the scheme in Table 3. The MrBayes analysis was computed with 2,000,000 generations of two iterations of four Markov chain Monte Carlo (MCMC) chains, where trees were sampled every 100 generations. Chain convergence was confirmed by both visualization by Tracer v. 1.7.2 (Rambaut et al. 2018) and a small value (< 0.01) of average standard deviation of split frequencies (ASDSF). After burn-in of the first 25% generations, the consensus topology was constructed based on the 50% majority-rule of whole topologies. We also constructed concatenated gene trees based on the RAxML and maximum-parsimony methods. The RAxML phylogeny was computed under the GTRGAMMAI substitution model with 1,000 replications of bootstraps. The maximum-parsimony trees were inferred by Subtree-Pruning-Regrafting (SPR) methods with 1,000 replications of bootstraps using MEGA 7 v. 0.26 (Kumar et al. 2016), and a bootstrap consensus tree was constructed from the resulting 10 unrooted trees.

Table 3
Optimal partitioning scheme and substitution models for MrBayes analysis using PartitionFinder 2.

Scheme nos.	Subsets *	Substitution model	Total sites including gaps	Base positions
1	ITS	GTR + G	520	1–246; 404–677
2	5.8S	K80 + I	157	247–403
3	28S	GTR + I + G	895	678–1572
4	*TEF1*-int, *RPB1*-int	GTR + I	157	1573–1586; 3368–3440; 3578–3647
5	*RPB1*-c1, *RPB2*-c1	GTR + I	561	1587–2470/3; 2471–3268/3
6	*RPB1*-c2, *RPB2*-c2	HKY	561	1588–2470/3; 2472–3268/3
7	*RPB1*-c3, *RPB2*-c3	GTR + G	560	1589–2470/3; 2473–3268/3
8	*TEF1*-c1, *TEF1*-c3	GTR + I + G	342	3269–3367/3; 3441–3577/3; 3648–3924/3; 3271–3367/3; 3443–3577/3; 3650–3924/3
9	*TEF1*-c2	HKY + I	171	3270–3367/3; 3442–3577/3; 3649–3924/3
				Total 3924 sites

* ITS, ITS1 and ITS2 regions. 5.8S and 28S, 5.8S and 28S of nc rDNA, respectively. C1, c2, and c3, first, second, and third positions of the coding region (*TEF1*, *RPB1*, and *RPB2*), respectively. Int, intronic regions of *TEF1*.

ITS1 and ITS2 regions were input as the same scheme. Three loci of *TEF1* intronic regions were input as the same scheme.

The alignments of ITS and concatenated dataset are provided in the Supplementary Data. Numerical information concerning the alignments (e.g., numbers of parsimony-informative sites and distinct alignment patterns) is shown in **Table S3**.

2.7. Species delimitations

Because there was a little conflict among topologies constructed from single alignments, we performed species delimitation using GCPSR (Taylor et al. 2000), GMYC (Pons et al. 2006), and BP&P (Yang 2002; Rannala and Yang 2003) approaches. The GCPSR approach defines a congruence of multi-gene genealogies as a phylogenetic species. In the GCPSR protocol proposed by Dettman et al. (2003, 2006), congruent clades were recognized as genealogical concordance and/or genealogical non-discordance; they were then defined as phylogenetic species via exhaustive subdivision, in which all individuals were required to be placed within a phylogenetic species without creating conflicts with other phylogenetic species. Here, genealogical concordance was defined as the same monophyletic clade recognized in most topologies (≥ 3 of 4 of ITS-LSU, *TEF1*, *RPB1*, and *RPB2* phylogenies); genealogical non-discordance was defined as the recognition of supported-monophyly (MLBS ≥

70) in ≥ 1 topology, the clustering of which is never contradicted with the same level of support in other topologies. Finally, specimens were defined as the smallest phylogenetic groups that did not create discordance.

The GMYC approach explores the switching of branching by speciation under the Yule model (interspecific) to neutral coalescent within a species (intraspecific) based on the topology of an ultrametric tree (Pons et al. 2006; Fujisawa and Barraclough 2013). The species delimitation based on GMYC was analyzed using "splits" package in R v. 4.0.5. We generated an ultrametric tree for each locus (ITS-LSU, *TEF1*, *RPB1*, and *RPB2*) under Bayesian inference implemented in BEAST 2 v. 6.6 (Bouckaert et al. 2019). We set a strict clock model for estimating branch lengths and tree priors under the Yule model. The MCMC analysis was performed for 10,000,000 generations and sampled every 1,000 steps. The convergence of chain was confirmed by higher values (≥ 200) of effective sample size (ESS) for each parameter on Tracer, and a consensus topology was summarized after a 25% burn-in. For each locus, we removed an outgroup (i.e., *Sistotrema* spp.) from the topology using "ape" package (Paradis and Schliep 2019) and assigned the topology by GMYC analysis with a single threshold using "splits" package (Thomas et al. 2021).

The BP&P is a Bayesian MCMC program that infers species tree and species delimitation under the multispecies coalescent model using multiple-locus alignments (Yang 2002; Rannala and Yang 2003). We performed an unguided species delimitation of "A11" algorithm in BP&P v. 4.3., which performs joint species delimitation and species tree inference using the reversible-jump MCMC algorithm (Yang and Rannala 2014). We assigned 26 individuals for four inferenced species as a prior (*H. repandum*, *H. boreorepandum*, ROC, and ROF); four alignments (ITS-LSU, *TEF1*, *RPB1*, *RPB2*) were assigned as multiple loci. Because we could not provide the corroborated values of the population size parameters (θs) and the divergence time at the root of the species tree (τ_0) for each inverse gamma distribution, we assigned four combinations of rate parameters between higher (0.1) and lower (0.01) values as a prior in multiple analyses (Košuthová et al. 2020); overall, "A11" analyses were independently run under priors [θs = 0.01 and τ_0 = 0.01], [θs = 0.01 and τ_0 = 0.1], [θs = 0.1 and τ_0 = 0.01], and [θs = 0.1 and τ_0 = 0.1]. The shape parameter 2 was assigned to each inverse gamma distribution. The remaining divergence parameters (τs) were assigned to the Dirichlet prior (Yang and Rannala 2010: Eq. 2). These analyses were run twice to confirm consistency between iterations.

The evolutionary divergences in each gene were analyzed to estimate overlapping of inter/intraspecific variations within/between each group. This analysis is useful for determining the optimal DNA barcode (e.g., Harder et al. 2013; Li et al. 2017; Wang et al. 2018). Using MEGA 7, the mean evolutionary divergence "within groups" and "net between groups" were estimated for each locus (ITS, LSU, *TEF1*, *RPB1*, and *RPB2*). The maximum-composite-likelihood method with 1,000 replications of bootstrap analysis was implemented to analyze pairwise distances. The patterns among lineages were set as gamma distribution rates, including site heterogeneity.

3. Results

3.1. Phylogenetic analyses

The RAxML phylogram obtained from the ITS dataset showed topology similar to the phylogram in our previous study (Fig. 2; Sugawara et al. 2022a). Sequences of ROC, ROF, *H. repandum*, and *H. boreorepandum* formed a monophyletic clade with strong support (MLBS = 93) within the subg. *Hydnum* (MLBS = 75). *Hydnum repandum* sequences formed a paraphyletic group with *H. boreorepandum* and *H. repando-orientale* s. lat. *Hydnum boreorepandum* including European and East Asian specimens showed monophyly with strong support (MLBS = 91). *Hydnum repando-orientale* s. lat. (i.e., the assemblage of ROC and ROF groups) formed a monophyletic clade with strong support (MLBS = 100). Among them, all 18 sequences in the ROF group, including holotype of *H. repando-orientale* (TUMH 60745), were slightly separated from the sequences in the ROC group as a subclade with low support (MLBS = 61). Three specimens in the ROC group formed a further subclade with the other eight sequences in the ROC group with moderate support (MLBS = 82).

Independent phylogenies of ITS-LSU, *TEF1*, *RPB1*, and *RPB2* showed slightly different topologies regarding the relationships among ROC, ROF, and *H. boreorepandum*. The ITS-LSU dataset showed a paraphyletic relationship between the ROC and ROF groups (MLBS = 100 in ROF + ROC; MLBS = 69 in ROF alone), corresponding to the ITS alone dataset described above (**Fig. S1**). The *TEF1* phylogeny had strong support for monophyly in each clade of *H. boreorepandum* (MLBS = 100) and ROC (MLBS = 95). Most ROF specimens formed a monophyletic clade, but one ROF specimen (TUMH 63126) was outside the ROC and ROF clades (**Fig. S2**). The *RPB1* phylogeny showed two monophyletic clades of ROC (MLBS = 99) and ROF (MLBS = 100), together with a paraphyletic position of *H. boreorepandum* (MLBS = 92); the assemblage of ROC and ROF groups formed a moderately supported clade (MLBS = 75) (**Fig. S3**). The *RPB2* phylogeny showed monophyletic clades of ROC (MLBS = 97), ROF (MLBS = 96), and *H. boreorepandum* (MLBS = 99); the assemblage of ROC and ROF groups formed a strongly supported clade (MLBS = 96; **Fig. S4**).

The Bayesian inference tree of the concatenated dataset showed that ROC, ROF, *H. boreorepandum*, and *H. repandum* specimens formed independent clades within the subg. *Hydnum* clade (Fig. 3). The maximum likelihood and maximum-parsimony trees were almost consistent with the Bayesian tree; thus, four species-level clades were supported by all approaches. The maximum likelihood bootstrap, maximum-

parsimony bootstrap (MPBS), and Bayesian inference posterior probability (BIP) values for each branch were 100/100/1 in ROC, 99/99/1 in ROF, 100/100/1 in *H. boreorepandum*, and 100/100/1 in *H. repandum*. In addition, the ROF clade has a subclade, comprising three specimens with moderate support (MLBS/MPBS/BIP = 71/96/0.99). ROC formed a sister clade of ROF (MLBS/MPBS/BIP = 100/100/1), and *H. boreorepandum* was positioned as a sister clade of the assemblage of ROC and ROF groups (MLBS/MPBS/BIP = 100/100/1).

3.2. Species delimitations

A summary of each species delimitation is shown in Fig. 4. The GCPSR criterion supported both genealogical concordance and non-discordance of ROC, ROF, and *H. boreorepandum*, respectively (see "C/nDC" on branches in Fig. 4). A subclade of the ROF group containing three specimens (TNS-F-78326, TUMH 63125, and TUMH 64069) exhibited genealogical non-discordance. Finally, the exhaustive subdivision process (Dettman et al. 2006) in the GCPSR approach recognized ROC, ROF, and *H. boreorepandum* as three phylogenetically distinct species and the subclade in ROF as an intraspecific variation.

The GMYC analyses of each topology rejected the null model (likelihood ratio test p-value < 0.001) and supported the assumption that all *H. boreorepandum* specimens belonged to a single group. The unity of a mixed group of ROC and ROF specimens was supported by the ITS-LSU topology (AICc-supported-value = 1.00) but not by the *TEF1*, *RPB1*, and *RPB2* topologies (< 0.15). ROC and ROF specimens were clearly separated as two distinct groups based on the *RPB1* and *RPB2* topologies. In the *TEF1* topology, most ROF and ROC specimens were assigned to distinct two groups; one ROF specimen (TUMH 63126) formed a separate group.

The BP&P analysis under all combinations of θs and τ_0 priors supported a four-species model composed of *H. boreorepandum*, *H. repandum*, ROC, and ROF, with the highest posterior probabilities (0.98–1.00). These analyses supported the assumption that the ROC and ROF groups were two distinct species with high posterior probability support (≥ 0.98) in the all priors set; they did not support a single species model for ROC and ROF. Therefore, all species delimitation approaches supported the assumption that ROC and ROF are distinct species, rather than a single species.

For all loci (ITS, LSU, *TEF1*, *RPB1*, and *RPB2*), the ranges of evolutionary divergences within each ecological group estimated by the maximum-composite-likelihood method were 0.000–0.001 in ROC, 0.000–0.004 in ROF, and 0.000–0.001 in *H. boreorepandum* (Table 4). The variation of ITS sequences among *H. boreorepandum*, ROC, and ROF was considerably higher (0.012–0.014) than in *H. boreorepandum* alone (0.000–0.001); however, the variation between ROC and ROF (0.001) overlapped with the variation within each group (0.000–0.001). Compared with ITS, LSU sequences showed lower values of evolutionary divergences in all groups; thus, three groups could not be distinguished by ITS and LSU markers. However, each of the *TEF1*, *RPB1*, and *RPB2* genes showed substantially higher variation among the three groups, compared to within the three groups: divergences of [single group vs. all three groups] were [≤ 0.004 vs. 0.008–0.019] in *TEF1*, [≤ 0.001 vs. 0.006–0.010] in *RPB1*, and [0.000 vs. 0.005–0.014] in *RPB2* (Table 4).

Table 4
Average evolutionary divergences within/between groups.

	Phylogenetic/ecological groups	ITS	LSU	*TEF1*	*RPB1*	*RPB2*
Within group	ROC	0.001	0.000	0.001	0.000	0.000
	ROF	0.000	0.000	0.004	0.000	0.000
	H. boreorepandum	0.001	0.001	0.000	0.001	0.000
Between group	ROC vs. ROF	0.002	0.000	**0.008**	**0.010**	**0.005**
	ROC vs. *H. boreorepandum*	0.015	0.002	0.019	0.006	0.014
	ROF vs. *H. boreorepandum*	0.017	0.002	0.019	0.007	0.014

The average evolutionary divergences estimated by the maximum-composite-likelihood method using MEGA 7. ROC and ROF showed higher interspecific divergences in *TEF1*, *RPB1* and *RPB2* (in bold), compared to ITS and LSU.

3.3. Morphological analysis

With the exception of basidiospore size, no diagnostic micro-macroscopic morphologic character could distinguish among ROC, ROF, and *H. boreorepandum*. The basidiospore length or width of three species overlapped; however, the MBS was slightly larger in the ROC group (Fig. 5): [ave. 8.0–9.1 × 6.9–8.0 µm, Q_m = 1.08–1.16] in ROC, [ave. 7.2–8.3 × 6.5–7.5 µm, Q_m = 1.09–1.17] in ROF (Sugawara et al. 2022a), and [ave. 7.8–8.7 × 6.9–7.3 µm, Q_m = 1.10–1.19] in *H. boreorepandum* (Sugawara et al. 2022a). Additionally, basidiospores of ROC specimens were slightly larger than basidiospores of *H. repandum* (ave. 7.3–8.4 × 6.2–7.1 µm; Grebenc et al. 2009; Olariaga et al. 2012; Niskanen et al. 2018). Pairwise Wilcoxon rank-sum tests showed that basidiospore length and width were significantly larger in ROC than ROF [p = 0.000 (L)/0.001

(W)] and *H. repandum* [$p = 0.005$ (L)/0.005 (W)] (**Table S4**). There was no significant difference between ROC and *H. boreorepandum* in terms of basidiospore length ($p = 0.368$), whereas ROC showed a significantly larger basidiospore width ($p = 0.019$).

3.4. Mating incompatibility tests

Because clamped hyphae were observed (although infrequently) compared to absent in the original simple-septate hyphae, mating compatibility was evaluated based on the presence of clamp connection at junctions between two confronting colonies. Mating tests showed mating compatibility exists in each ecological/phylogenetic group (Table 5). Although most strains did not show mating compatibility with a strain of a different group, two strains showed mating compatibility beyond their potential incompatibility group (Table 5): one ROC strain (SuR20200920-007 ST03: TUMH 60412) formed clamps with all ROF strains, and one *H. boreorepandum* strain (SuR20201011-301 ST03: TUMH 64408) formed clamps with several ROF strains (**Fig. S5**). The clamped hyphae between ROC and ROF strains showed dikaryotization of hyphal cells (**Fig. S5e**), and we successfully isolated it as a dikaryotic culture strain (SuR20201024-101 ST01 × SuR20200920-007 ST03). Because the clamped hyphae generated by crossing of *H. boreorepandum* and ROF strains were very rare and sparse, their nuclear phase could not be observed and they could not be isolated in culture; we thus presumed that their dikaryotization failed or the dikaryon lost viability on culture medium. In conclusion, ROF, ROC, and *H. boreorepandum* groups belong to different mating incompatibility groups but retain partial mating ability; one ROC strain potentially has the ability to form a hybrid with ROF; one *H. boreorepandum* strain contingently forms clamp-like structures by crossing with ROF but has the lost normal mating ability.

3.5. Taxonomy

Hydnum L. subg. *Hydnum* L.

Hydnum L. sect. *Hydnum* L.

Hydnum subalpinum R. Sugaw. & N. Endo, sp. nov. Figure 6.

MycoBank no.: 844782

Diagnosis: *Hydnum subalpinum* is a sister species of *H. repando-orientale* but differs in that its basidiospores are slightly larger (8–10 × 6.5–8.5 µm) and it occurs in subalpine forest habitats associated with Gymnosperm. This species is also related to *H. boreorepandum*: *H. subalpinum* and *H. boreorepandum* show similar morphologies and ecologies but differs in terms of phylogeny and biological isolation, as indicated by *in vitro* mating incompatibility.

Type

JAPAN, Nagano Pref., Chino City, Tsuboniwa, 2250 m, on the ground under *Abies homolepsis*, *Tsuga diversifolia*, and *Pinus pumila* individuals, 26 Sep 2020, *R. Sugawara SuR20200926-002* (TUMH 64016); ex-holotype culture, TUFC XXXX (monosporous strain).

Gene sequences ex-holotype

LC621871 (ITS), LC717891 (LSU), LC622497 (*TEF1*), LC717817 (*RPB1*), LC717851 (*RPB2*)

Etymology: *subalpinum*, from its distribution range.

Japanese name

Takane-kanoshita

Macroscopic characters

Basidiomata medium to large-sized, 5–10 cm high, robust, solitary or gregarious. Pileus 3–7.5 cm diam, round to reniform, convex to plano-convex, infundibuliform when old; surface glabrous, smooth, sometimes depressed at center; whitish cream, cream to pale yellow (4A2–4A6), partly tinged yellowish orange (4A8), sometimes coloring orange ochraceous (6B6–8); margin incurved when young, becoming straight to undulant, concolor to surface. Spines conical to spathulate, slightly distant, up to 9 mm long, whitish cream to cream (4A2–4A4), adnate to clearly decurrent. Stipe robust, 20–60 × 9–16 mm, central or eccentric, equal to slightly enlarged at the base, solid, glabrous, whitish cream to cream, not turning color where scratched. Context flesh, whitish cream to cream, when young turning yellowish where scratched. Rhizomorphs abundant, white. Odor mild, strong.

Microscopic characters

Basidiospores (7.5)7.7–9.8(10.4) × (6.1)6.5–8.6(9.4) µm, Q = (1.00)1.03–1.23(1.32), Q_m = 1.08–1.16 [mean, 8.0–9.1 × 6.9–8.0 µm, Q_m = 1.11], thin-walled, smooth, subglobose to broadly ellipsoid, hyaline in 3% KOH, containing subhyaline oily droplets, inamyloid. Basidia 36.5–66 × 7.5–12 µm, 3–5-spored, clavate to suburniform, thin-walled, smooth, including subhyaline oily droplets, sterigma 3.5–7.5 µm long. Hyphae of spines 2.5–4.5 µm wide, thin-walled, smooth, hyaline, sometimes including brownish cytoplasmic pigment; hyphal end cylindric to clavate, 3–7 µm wide. Pileipellis mixocutis, subhyaline; hyphae 5–10 µm wide, cylindric to slightly inflate at apex. Stipitipellis mixocutis, subhyaline; hyphae 3–4.5 µm wide, cylindric, without colored pigment. Cystidium absent. Rhizomorphs composed of hyphae 2.5–5.5 µm wide, cylindric, thin-walled, smooth, containing subhyaline oily droplets, including ampullate inflation at hyphal septum, 5.5–8 µm wide. Clamp connection present in all tissues.

Ecology and distribution

On ground in conifer-dominated forest of *Abies*, *Pinus*, and *Tsuga*, including some *Betula* in subalpine climate (1900–2500 m a.s.l.). High mountain in Nagano and Yamanashi Pref. in Japan.

Additional specimens examined: JAPAN. Nagano Pref.: Minamisaku Dist., Sakuho Town, Maruyama, 2180 m, under *Abies mariesii* in coniferous forest of *Abies*, *Tsuga*, *Pinus* with some *Betula*, 23 Sep 2020, *R. Sugawara SuR20200923-101* (TUMH 64014); 2100 m, under *A. mariesii* near *Abies* and *Tsuga* trees, 23 Sep 2020, *R. Sugawara SuR20200923-202* (TUMH 64015); Kawakami Village, Jumonjitoge, 2000 m, under *T. diversifolia*, 1 Oct 2019, *W. Aoki SuR20191130-02* (TUMH 64011); *Kitayokodake*, under *A. mariesii*, 9 Sep 2020, *W. Aoki SuR20201121-201* (TUMH 64017); Mount Aka, 2400 m, in fir forest of *A. mariesii*, 20 Sep 2020, *R. Sugawara SuR20200920-007* (TUMH 64012); *R. Sugawara SuR20200920-012* (TUMH 64013); 2500 m, in fir forest of *A. mariesii*, 20 Sep 2020, *R. Sugawara SuR20200920-012* (TUMH 64013); Toyohira, 2070 m, in coniferous forest of *P. koraiensis*, *A. veitchii*, *T. diversifolia*, 1 Sep 2021, *A. Koyama SuR20210907-002* (TUMH 64030); Suwa Dist., Fujimi Town, Mount Kamanashi, 1890 m, on the ground in *A. veitchii* dominated forest with some *T. diversifolia* and *Betula ermanii*, 3 Sep 2021, *A. Koyama SuR20210907-001* (TUMH 64029). Yamanashi Pref.: Minamitsuru Dist., Narusawa Village, Okuniwa, 2200 m, in mixed forest of *B. ermanii*, *T. diversifolia*, and *A. mariesii*, 20 Sep 2018, *E. Imura 199* (TNS-F-85326, labeled as "*Hydnum rufescens*"); Minami-Alps City, Kitazawatoge, 2000 m, 28 Aug 2017, *H. Uehara 122* (TNS-F-80714, labeled as "*Hydnum rufescens*").

Remarks: *Hydnum subalpinum* morphologically resembles most species in the subg. *Hydnum*; namely, *H. boreorepandum*, *H. olympicum*, *H. repando-orientale*, *H. repandum*, *H. slovenicum*, *H. vagabundum*, and *H. washingtonianum*. Of these eight species, *H. boreorepandum*, *H. repando-orientale*, and *H. subalpinum* can be found in Japan; therefore, the remaining five species were distinguished by their geographic distributions in Europe and Northern to Southern America (see Fig. 2). Morphological differences among these species were very poor; however, *H. subalpinum* shows the largest basidiospores along with *H. olympicum* (8.0–9.2 × 6.5–7.5 µm; Niskanen et al. 2018). *Hydnum sphaericum* is a Chinese species in the subg. *Hydnum* but differs in a smaller pileus (20–35 mm wide) and slightly narrower basidiospores [(6.0)6.5–7.5(8.0) µm wide, Q_m = 1.20–1.23; Cao et al. 2021b]. The most diagnostic feature of *H. subalpinum* is the forest habitat, where they occur in conifer-dominated subalpine forest located at high elevation (> 1900 m) in Japan. Compared to other species in this subgenus, *H. sphaericum*, *H. subolympicum*, and *H. repando-orientale* occur in broadleaved forests, whereas *H. boreorepandum*, *H. olympincum*, *H. slovenicum*, and *H. washingtonianum* occur in coniferous forests (Niskanen et al. 2018; Swenie et al. 2018; Cao et al. 2021b; Sugawara et al. 2022a). *Hydnum boreorepandum* and *H. subalpinum* cannot be distinguished by morphology or forest habitats, but all genomic DNA markers support their distinct biological isolation.

Pileal color of *H. boreorepandum* and *H. subalpinum* was slightly whiter, compared with *H. repandum* and *H. repando-orientale* (Niskanen et al. 2018; Sugawara et al. 2021a); we presumed that this was affected by environmental condition. Indeed, older basidiomata of *H. boreorepandum* were tinged with orange hues (Sugawara et al. 2021a). This notation is supported by two TNS specimens of *H. subalpinum* that were labeled as "*H. rufescens*" in the subg. *Rufescentia* Niskanen & Liimat. because of their brownish-orange color. Yanaga et al. (2015) showed that *H. repando-orientale* (as "*H. repandum* var. *repandum*" and "*H. repandum* var. *album*") has color variations of the pileus, even at the same collection site.

5. Discussion

In this study, integrative taxonomic approaches verified that two ecological groups of *H. repando-orientale* s. lat. constituted two independent species. Phylogeny inferred from five loci demonstrated the distinct divergence between temperate ROF (*H. repando-orientale*) and subalpine ROC (*H. subalpinum*) groups. While *H. repando-oriental* and *H. subalpinum* have not yet accumulated sufficient variations in ITS, LSU, and *TEF1*, all species delimitation analyses (GCPSR, GMYC, and BP&P) separated them into two distinct phylogenetic clades; this genetic divergence implies reproductive isolation derived from their different ecological niches. Contrary to our expectations, mating tests among monospore isolates in these two species did not show complete incompatibility between species—one strain showed intermediate incompatibility. However, the other strains exhibited mating incompatibility with other species. Morphological difference between these two species are scarce, but *H. subalpinum* specimens have significantly larger basidiospores, compared with specimens of *H. repando-orientale*. We

suspect that these two species have lost gene flow because of local adaptation to different vegetation/climate conditions; genetic divergence accumulated independently, resulting in mating incompatibility and phenotypic differences.

One strain of *H. subalpinum* (SuR20200920-007 ST03: TUMH 64012) clearly showed *in vitro* dikaryotization with *H. repando-orientale* strains. This hybridization ability indicates recent speciation into *H. repando-orientale* and *H. subalpinum*. However, although the sister species have not established genetic hybrid incompatibility, they presumably have other isolating barriers such as immigrant inviability or ecological hybrid inviability (Nosil et al. 2005) because of their allopatric distribution and niche divergence. In many basidiomycetes, the crossing of different species is frequently observed in mating tests (Le Gac and Giraud 2008). A typical case is that of *Flammulina* species (e.g., *F. filiformis*, *F. velutipes*, and *F. rossica*); they show incomplete reproductive isolation in mating tests (Petersen et al. 1999; Ripková et al. 2010), but natural basidiomata retain an independent monophyletic lineage and have a separate genetic structure in each species (Wang et al. 2018). Evidence of hybridization is occasionally detected in natural basidiomata as interspecific heterozygosity (Garbelotto et al. 1996; Hughes and Petersen 2001; Kauserud et al. 2007; Ripková et al. 2010; Harder et al. 2013; Hughes et al. 2013; Li et al. 2017; Sillo et al. 2019). However, in most cases, F_1 hybrids rarely occur in nature because their low hybrid viability hinders the production of F_2 or higher progeny (Hughes et al. 2013). Therefore, the hybridization among close species is occasionally observed in basidiomycetes when the potential pre/post-zygotic isolation events do not occur. In this study, crossing between *H. repando-orientale* and *H. subalpinum* was probably an artifact of the unnatural *in vitro* conditions, which enforces mating between ecologically allopatric species.

Another case that suggests stable natural hybridization in basidiomycetes was reported from *Heterobasidion irregulare* Garbel. & Otrosina and *H. occidentale* Otrosina & Garbel., plant pathogens in the order *Russulales* (Garbelotto et al. 1996; Garbelotto and Gonthier 2013; Sillo et al. 2019). *Heterobasidion irregulare* and *H. occidentale* have distinct host ranges but a parapatric to sympatric distribution in North America (Otrosina and Garbelotto 2010; Garbelotto and Gonthier 2013). These two species can easily cross in nature and *in vitro*, and fruiting of the natural hybrid occurs on intermediate host plants. In this case, repeated backcrossing has caused *H. irregulare*, *H. occidentale*, and its hybrids to have greater genetic variations in their fungal DNA [ITS, *TEF1*, *RPB2*, and glyceraldehyde-3-phosphate dehydrogenase (*GPD*)] because of the recombination of different alleles from distinct species (Sillo et al. 2019). In the present study, *H. repando-orientale* and *H. subalpinum* showed lower intraspecific genetic variations, supporting the notion of minimal gene flow between the two populations. Furthermore, mating incompatibility among most *H. repando-orientale* and *H. subalpinum* strains indicates deeper reproductive isolation by genetic drift. This rapid generation of hybrid incompatibility is explained as reinforcement between different ecological populations (Dobzhansky 1940; Noor 1999).

We also clarified the species boundaries of *H. repandum*, *H. boreorepandum*, and *H. repando-oreintale*. *Hydnum boreorepandum* and *H. subalpinum* co-occur in the same forests; however, they showed hybrid incompatibility and clear intra/interspecific evolutionary divergence in all genomic markers (Table 4). Furthermore, each species delimitation approach recognized *H. boreorepandum* as a single species separate from *H. repando-orientale* s. lat. Therefore, our findings support strict species boundaries among *H. boreorepandum*, *H. repando-orientale*, *H. repandum*, and *H. subalpinum*, despite smaller interspecific variations in ITS sequences (1%; Niskanen et al. 2018). The ITS sequences do not indicate a convincing topology between *H. repandum* and related species; notably, *H. repando-orientale* and *H. subalpinum* show overlapping intra/interspecific variations in ITS and LSU sequences. Thus, these nc rDNA markers are unsuitable for species delimitation and identification for the subg. *Hydnum*. Alternatively, *RPB1* and *RPB2* sequences enabled phylogenetic delimitation among *H. boreorepandum*, *H. repando-orientale*, and *H. subalpinum*. The *RPB2* primers designed here enabled PCR amplification of all Japanese *Hydnum* and mycorrhizal *Sistotrema* species; therefore, we recommend use of the *RPB2* gene fragment as the second DNA barcode for this genus. The *RPB1* gene is also a useful molecular marker to identify this taxon, but the *RPB1* primers for *Hydnum* designed by Feng et al. (2016) did not enable PCR amplification of some *Hydnum* and *Sistotrema* species.

The concatenated phylogeny strongly indicates that *H. boreorepandum*, *H. repando-orientale*, *H. repandum*, and *H. subalpinum* share a common ancestor, which might have experienced speciation in relation to geographic isolation along with adaptation to host and temperature. Additionally, *H. repandum* and its closely related species have more informative taxonomic characteristics in terms of ecogeographical traits (geographic distribution, temperature of habitat, and host association), rather than morphology. *Hydnum washingtonianum*, a sister clade of these four species, also has the diagnostic ecogeography of a North American distribution and coniferous forest habitats (Niskanen et al. 2018; Swenie et al. 2018). In contrast, there have been few revelations concerning the biogeography of most lineages in subg. *Hydnum*. The biogeographic history of this taxon can provide insight into the worldwide dispersal and diversification of ectomycorrhizal species in *Agaricomycetes*. To understand the biogeography of species in the subg. *Hydnum*, there is a need for species identification and delimitation using integrative approaches, including multiple DNA markers, ecogeographical information, morphological analysis, and mating incompatibility testing.

Declarations

Acknowledgments

We thank Dr. K. Hosaka (Department of Botany, Division of Fungi and Algae, National Museum of Nature and Science, Tokyo) for the loan of specimens from the National Museum of Nature and Science (TNS); the Nagano Prefectural Government, the ministry of the Environment, and the Forestry Agency of Japan for the permissions of field research in special protection zones. We also thank A. Koyama and M. Shishikura for donation of the basidiomata collections and digital photographs. We thank the DNA Data Bank of Japan for nucleotide sequence submission; Fasmac Co., Ltd for technical support regarding DNA sequencing. This research was financially supported by JSPS KAKENHI Grant Number JP20J20884 (Ryo Sugawara) from Japan Society for the Promotion of Science.

Authors' contribution

Ryo Sugawara, Naoki Endo, and Akira Nakagiri contributed to the study conception and design. Materials preparation was performed by Ryo Sugawara, Naoki Endo, Wataru Aoki, and Akiyoshi Yamada. Data collection and analyses were performed by Ryo Sugawara. The original draft of the manuscript was written by Ryo Sugawara and all authors commented on previous versions of the manuscript. All authors read and approved the final manuscript.

Funding

This research was supported by JSPS KAKENHI Grant Number JP20J20884 (Ryo Sugawara) from Japan Society for the Promotion of Science.

Data availability

Voucher specimens and culture collections have been deposited in the Tottori University Mycological Herbarium (TUMH), Fungus/Mushroom Resource and Research Center, Faculty of Agriculture, Tottori University University. The newly generated sequences have been submitted in INSD with the accession numbers listed in **Tables 2 and S2**. The alignments for phylogenetic analyses are provided in Supplementary Data. All other data generated or analyzed in this research available from the corresponding author on requests.

Ethics approval and consent to participate Not applicable

Consent for publication Not applicable

Competing interests The authors declare no competing interests.

References

1. Abarenkov K, Tedersoo L, Nilsson RH et al (2010) PlutoF—a web based workbench for ecological and taxonomic research, with an online implementation for fungal ITS sequences. Evol Bioinforma 6. https://doi.org/10.4137/EBO.S6271. EBO.S6271
2. Aime MC, Miller AN, Aoki T et al (2021) How to publish a new fungal species, or name, version 3.0. IMA Fungus 12:11. https://doi.org/10.1186/s43008-021-00063-1
3. Asahina Y (1939) Illustrations of Japanese Cryptogams (in Japanese). Sanseido, Tokyo, Japan
4. Bengtsson-Palme J, Ryberg M, Hartmann M et al (2013) Improved software detection and extraction of ITS1 and ITS2 from ribosomal ITS sequences of fungi and other eukaryotes for analysis of environmental sequencing data. Methods Ecol Evol 4:914–919. https://doi.org/https://doi.org/10.1111/2041-210X.12073
5. Bouckaert R, Vaughan TG, Barido-Sottani J et al (2019) BEAST 2.5: An advanced software platform for Bayesian evolutionary analysis. PLOS Comput Biol 15:e1006650
6. Cao B, Haelewaters D, Schoutteten N et al (2021a) Delimiting species in Basidiomycota: a review. Fungal Divers 109:181–237. https://doi.org/10.1007/s13225-021-00479-5
7. Cao T, Hu Y-P, Yu J-R et al (2021b) A phylogenetic overview of the Hydnaceae (Cantharellales, Basidiomycota) with new taxa from China. Stud Mycol 99:100121. https://doi.org/https://doi.org/10.1016/j.simyco.2021.100121
8. Coker WC, Beers AH (1951) The stipitate Hydnums of the Eastern United States. Oxford University Press., London, United Kingdom
9. Darriba D, Posada D, Kozlov AM et al (2020) ModelTest-NG: A new and scalable tool for the selection of DNA and protein evolutionary models. Mol Biol Evol 37:291–294. https://doi.org/10.1093/molbev/msz189
10. Dettman JR, Jacobson DJ, Taylor JW (2003) A multilocus genealogical approach to phylogenetic species recognition in the model *Eukaryote neurospora*. Evolution 57:2703–2720. https://doi.org/https://doi.org/10.1111/j.0014-3820.2003.tb01514.x

11. Dettman JR, Jacobson DJ, Taylor JW (2006) Multilocus sequence data reveal extensive phylogenetic species diversity within the *Neurospora discreta* complex. Mycologia 98:436–446. https://doi.org/10.1080/15572536.2006.11832678
12. Dobzhansky T (1940) Speciation as a stage in evolutionary divergence. Am Nat 74:312–321. https://doi.org/10.1086/280899
13. Edler D, Klein J, Antonelli A, Silvestro D (2021) raxmlGUI 2.0: A graphical interface and toolkit for phylogenetic analyses using RaxML. Methods Ecol Evol 12:373–377. https://doi.org/10.1111/2041-210X.13512
14. Feng B, Wang XH, Ratkowsky D et al (2016) Multilocus phylogenetic analyses reveal unexpected abundant diversity and significant disjunct distribution pattern of the Hedgehog Mushrooms (*Hydnum* L.). Sci Rep 6:1–11. https://doi.org/10.1038/srep25586
15. Flouri T, Izquierdo-Carrasco F, Darriba D et al (2015) The phylogenetic likelihood library. Syst Biol 64:356–362. https://doi.org/10.1093/sysbio/syu084
16. Fujisawa T, Barraclough TG (2013) Delimiting species using single-locus data and the generalized mixed Yule coalescent approach: A revised method and evaluation on simulated data sets. Syst Biol 62:707–724. https://doi.org/10.1093/sysbio/syt033
17. Fujita MK, Leaché AD, Burbrink FT et al (2012) Coalescent-based species delimitation in an integrative taxonomy. Trends Ecol Evol 27:480–488. https://doi.org/https://doi.org/10.1016/j.tree.2012.04.012
18. Garbelotto M, Gonthier P (2013) Biology, epidemiology, and control of *Heterobasidion* species worldwide. Annu Rev Phytopathol 51:39–59. https://doi.org/10.1146/annurev-phyto-082712-102225
19. Garbelotto M, Ratcliff A, Bruns TD et al (1996) Use of taxon-specific competitive-priming PCR to study host specificity, hybridization, and intergroup gene flow in intersterility groups of *Heterobasidion annosum*. Phytopathology 86:543–551. https://doi.org/10.1094/Phyto-86-543
20. Garbelotto M, Slaughter G, Popenuck T et al (1997) Secondary spread of *Heterobasidion annosum* in white fir root-disease centers. Can J For Res 27:766–773. https://doi.org/10.1139/x96-193
21. Gardes M, Bruns TD (1993) ITS primers with enhanced specificity for basidiomycetes – application to the identification of mycorrhizae and rusts. Mol Ecol 2:113–118. https://doi.org/10.1111/j.1365-294X.1993.tb00005.x
22. Grebenc T, Martín MP, Kraigher H (2009) Ribosomal ITS diversity among the European species of the genus *Hydnum* (Hydnaceae). An del Jardín. Botánico Madrid 66:121–132. https://doi.org/10.3989/ajbm.2221
23. Hall D, Stuntz DE (1971) Pileate Hydnaceae of the Puget Sound Area. I. White-spored genera: *Auriscalpium*, *Hericium*, *Dentinum* and *Phellodon*. Mycologia 63:1099–1128. https://doi.org/10.1080/00275514.1971.12019214
24. Harder CB, LæssØe T, FrØslev TG et al (2013) A three-gene phylogeny of the *Mycena pura* complex reveals 11 phylogenetic species and shows ITS to be unreliable for species identification. Fungal Biol 117:764–775. https://doi.org/10.1016/j.funbio.2013.09.004
25. Harrison KA, Grund DW (1987) Preliminary keys to the terrestrial stipitate Hydnums of North America. Mycotaxon 28:419–426
26. Hughes KW, Petersen RH (2001) Apparent recombination or gene conversion in the ribosomal ITS region of a *Flammulina* (Fungi, Agaricales) hybrid. Mol Biol Evol 18:94–96. https://doi.org/10.1093/oxfordjournals.molbev.a003724
27. Hughes KW, Petersen RH, Lodge DJ et al (2013) Evolutionary consequences of putative intra-and interspecific hybridization in agaric fungi. Mycologia 105:1577–1594. https://doi.org/10.3852/13-041
28. Imazeki R, Hongo T (1957) Coloured illustrations of fungi of Japan (in Japanese). Hoikusha, Osaka, Japan
29. Ito S (1955) Mycological flora of Japan, vol 2, 4 edn. Yokendo, Tokyo, Japan. (in Japanese)
30. Katoh K, Rozewicki J, Yamada KD (2019) MAFFT online service: multiple sequence alignment, interactive sequence choice and visualization. Brief Bioinform 20:1160–1166. https://doi.org/10.1093/bib/bbx108
31. Kauserud H, Hofton TH, Sætre G-P (2007) Pronounced ecological separation between two closely related lineages of the polyporous fungus *Gloeoporus taxicola*. Mycol Res 111:778–786. https://doi.org/https://doi.org/10.1016/j.mycres.2007.03.005
32. Kawamura S (1913) Illustrations of Japanese fungi, 2nd edn. The Bureau of Forestry, Ministry of Agriculture and Commerce, Tokyo, Japan
33. Kawamura S (1929) The Japanese fungi (in Japanese). Daichi-shoin, Tokyo, Japan
34. Kawamura S (1954) Icons of Japanese fungi (in Japanese), vol 4. Kazamashobo, Tokyo, Japan
35. Kikuhara N (1987) The Corticiales and Clavariales of Japan (in Japanese). Seichiken, Tokyo, Japan
36. Košuthová A, Bergsten J, Westberg M, Wedin M (2020) Species delimitation in the cyanolichen genus *Rostania*. BMC Evol Biol 20:115. https://doi.org/10.1186/s12862-020-01681-w
37. Kretzer AM, Bruns TD (1999) Use of *atp6* in fungal phylogenetics: An example from the Boletales. Mol Phylogenet Evol 13:483–492. https://doi.org/https://doi.org/10.1006/mpev.1999.0680
38. Kumar S, Stecher G, Tamura K (2016) MEGA7: Molecular evolutionary genetics analysis version 7.0 for bigger datasets. Mol Biol Evol 33:1870–1874. https://doi.org/10.1093/molbev/msw054

39. Lanfear R, Calcott B, Ho SYW, Guindon S (2012) PartitionFinder: Combined selection of partitioning schemes and substitution models for phylogenetic analyses. Mol Biol Evol 29:1695–1701. https://doi.org/10.1093/molbev/mss020
40. Lanfear R, Frandsen PB, Wright AM et al (2017) PartitionFinder 2: new methods for selecting partitioned models of evolution for molecular and morphological phylogenetic analyses. Mol Biol Evol 34:772–773. https://doi.org/10.1093/molbev/msw260
41. Le Gac M, Giraud T (2008) Existence of a pattern of reproductive character displacement in Homobasidiomycota but not in Ascomycota. J Evol Biol 21:761–772. https://doi.org/https://doi.org/10.1111/j.1420-9101.2008.01511.x
42. Li J, He X, Liu X-B et al (2017) Species clarification of oyster mushrooms in China and their DNA barcoding. Mycol Prog 16:191–203. https://doi.org/10.1007/s11557-016-1266-9
43. Linnaeus C (1753) Species plantarum: exhibentes plantas rite cognitas ad genera relatas, cum diferentiis specificis, nominibus trivialibus, synonymis selectis, locis natalibus, secundum systema sexuale digestas. Impensis Laurentii Salvii, Stockholm, Sweden, p 1178
44. Liu YJ, Whelen S, Hall BD (1999) Phylogenetic relationships among ascomycetes: evidence from an RNA polymerase II subunit. Mol Biol Evol 16:1799–1808. https://doi.org/10.1093/oxfordjournals.molbev.a026092
45. Liu YJ, Hodson MC, Hall BD (2006) Loss of the flagellum happened only once in the fungal lineage: phylogenetic structure of Kingdom Fungi inferred from RNA polymerase II subunit genes. BMC Evol Biol 6:74. https://doi.org/10.1186/1471-2148-6-74
46. Looney BP, Adamčík S, Matheny PB (2020) Coalescent-based delimitation and species-tree estimations reveal Appalachian origin and Neogene diversification in *Russula* subsection *Roseinae*. Mol Phylogenet Evol 147:106787. https://doi.org/https://doi.org/10.1016/j.ympev.2020.106787
47. Lücking R, Aime MC, Robbertse B et al (2020) Unambiguous identification of fungi: where do we stand and how accurate and precise is fungal DNA barcoding? IMA Fungus 11:14. https://doi.org/10.1186/s43008-020-00033-z
48. Maas Geesteranus RA (1971) Hydnaceous Fungi of the Eastern Old World. North-Holland Publishing Company, Amsterdam, London, United Kingdom
49. Matheny PB, Wang Z, Binder M et al (2007) Contributions of *rpb2* and *tef1* to the phylogeny of mushrooms and allies (Basidiomycota, Fungi). Mol Phylogenet Evol 43:430–451. https://doi.org/https://doi.org/10.1016/j.ympev.2006.08.024
50. Niskanen T, Liimatainen K, Nuytinck J et al (2018) Identifying and naming the currently known diversity of the genus *Hydnum*, with an emphasis on European and north American taxa. Mycologia 110:890–918. https://doi.org/10.1080/00275514.2018.1477004
51. Noor MAF (1999) Reinforcement and other consequences of sympatry. Heredity 83:503–508. https://doi.org/10.1038/sj.hdy.6886320
52. Nosil P, Vines TH, Funk DJ (2005) Reproductive isolation caused by natural selection against immigrants from divergent habitats. Evolution 59:705–719. https://doi.org/https://doi.org/10.1111/j.0014-3820.2005.tb01747.x
53. Olariaga I, Grebenc T, Salcedo I, Martín MP (2012) Two new species of *Hydnum* with ovoid basidiospores: *H. ovoideisporum* and *H. vesterholtii*. Mycologia 104:1443–1455. https://doi.org/10.3852/11-378
54. Otrosina WJ, Garbelotto M (2010) *Heterobasidion occidentale* sp. nov. and *Heterobasidion irregulare* nom. nov.: A disposition of North American *Heterobasidion* biological species. Fungal Biol 114:16–25. https://doi.org/https://doi.org/10.1016/j.mycres.2009.09.001
55. Paradis E, Schliep K (2019) ape 5.0: an environment for modern phylogenetics and evolutionary analyses. R Bioinf 35:526–528. https://doi.org/10.1093/bioinformatics/bty633
56. Petersen RH, Hughes KW, Redhead SA et al (1999) Mating systems in the Xerulaceae (Agaricales, Basidiomycotina): *Flammulina*. Mycoscience 40:411–426. https://doi.org/10.1007/BF02464396
57. Phillips R (2005) Mushrooms and Other Fungi of North America. Firefly Books, New York
58. Pons J, Barraclough TG, Gomez-Zurita J et al (2006) Sequence-based species delimitation for the DNA taxonomy of undescribed insects. Syst Biol 55:595–609. https://doi.org/10.1080/10635150600852011
59. R Core Team (2021) R: A language and environment for statistical computing. https://www.r-project.org/
60. Rambaut A, Drummond AJ, Xie D et al (2018) Posterior summarization in Bayesian phylogenetics using Tracer 1.7. Syst Biol 67:901–904. https://doi.org/10.1093/sysbio/syy032
61. Rannala B, Yang Z (2003) Bayes estimation of species divergence times and ancestral population sizes using DNA sequences from multiple loci. Genetics 164:1645–1656. https://doi.org/10.1093/genetics/164.4.1645
62. Rea C (1922) British Basidiomycetae: A handbook to the larger British Fungi. Cambridge University Press, France
63. Ripková S, Hughes K, Adamčík S et al (2010) The delimitation of *Flammulina fennae*. Mycol Prog 9:469–484. https://doi.org/10.1007/s11557-009-0654-9
64. Roberts P, Evans S (2011) The Book of Fungi. University of Chicago Press, Illinois, USA
65. Ronquist F, Teslenko M, van der Mark P et al (2012) MrBayes 3.2: Efficient Bayesian phylogenetic inference and model choice across a large model space. Syst Biol 61:539–542. https://doi.org/10.1093/sysbio/sys029

66. Sillo F, Gonthier P, Lockman B et al (2019) Molecular analyses identify hybridization-mediated nuclear evolution in newly discovered fungal hybrids. Ecol Evol 9:6588–6605. https://doi.org/https://doi.org/10.1002/ece3.5238
67. Stamatakis A (2014) RAxML version 8: a tool for phylogenetic analysis and post-analysis of large phylogenies. Bioinformatics 30:1312–1313. https://doi.org/10.1093/bioinformatics/btu033
68. Sugawara R, Yamada A, Kawai M et al (2019) Establishment of monokaryotic and dikaryotic isolates of Hedgehog mushrooms (*Hydnum repandum* and related species) from basidiospores. Mycoscience 60:201–209. https://doi.org/10.1016/j.myc.2019.02.007
69. Sugawara R, Maekawa N, Sotome K et al (2022a) Systematic revision of *Hydnum* species in Japan. Mycologia 114:413–452. https://doi.org/10.1080/00275514.2021.2024407
70. Sugawara R, Shirasuka N, Yamamoto T et al (2022b) Two new species of *Sistotrema* s.l. (Cantharellales) from Japan with descriptions of their ectomycorrhizae. Mycoscience 63:102–117. https://doi.org/10.47371/mycosci.2022.02.003
71. Swenie RA, Baroni TJ, Matheny PB (2018) Six new species and reports of *Hydnum* (Cantharellales) from eastern North America. MycoKeys 72:35–72. https://doi.org/10.3897/mycokeys.42.27369
72. Taylor JW, Jacobson DJ, Kroken S et al (2000) Phylogenetic species recognition and species concepts in fungi. Fungal Genet Biol. https://doi.org/10.1006/fgbi.2000.1228
73. Tedersoo L, Jairus T, Horton BM et al (2008) Strong host preference of ectomycorrhizal fungi in a Tasmanian wet sclerophyll forest as revealed by DNA barcoding and taxon-specific primers. New Phytol 180:479–490. https://doi.org/10.1111/j.1469-8137.2008.02561.x
74. Thomas E, Fujisawa T, Barraclough T(2021) splits: SPecies' LImits by Threshold Statistics. R package version 1.0–20/r56. https://r-forge.r-project.org/projects/splits/%0A
75. Thompson JD, Higgins DG, Gibson TJ (1994) CLUSTAL W: improving the sensitivity of progressive multiple sequence alignment through sequence weighting, position-specific gap penalties and weight matrix choice. Nucleic Acids Res 22:4673–4680. https://doi.org/10.1093/nar/22.22.4673
76. Wang PM, Liu XB, Dai YC et al (2018) Phylogeny and species delimitation of *Flammulina*: taxonomic status of winter mushroom in East Asia and a new European species identified using an integrated approach. Mycol Prog 17:1013–1030. https://doi.org/10.1007/s11557-018-1409-2
77. Yamada A, Katsuya K (1995) Mycorrhizal association of isolates from sporocarps and ectomycorrhizas with *Pinus densiflora* seedlings. Mycoscience 36:315–323. https://doi.org/10.1007/BF02268607
78. Yanaga K (2015) Taxonomic study of the order Cantharellales (Basidiomycota) in Japan (in Japanese). United Graduate School of Agricultural Sciences
79. Yanaga K, Sotome K, Ushijima S, Maekawa N (2015) *Hydnum* species producing whitish basidiomata in Japan. Mycoscience 56:434–442. https://doi.org/10.1016/j.myc.2015.01.001
80. Yang Z (2002) Likelihood and Bayes estimation of ancestral population sizes in Hominoids using data from multiple loci. Genetics 162:1811–1823. https://doi.org/10.1093/genetics/162.4.1811
81. Yang Z (2015) The BPP program for species tree estimation and species delimitation. Curr Zool 61:854–865. https://doi.org/10.1093/czoolo/61.5.854
82. Yang Z, Rannala B (2010) Bayesian species delimitation using multilocus sequence data. Proc Natl Acad Sci 107:9264–9269. https://doi.org/10.1073/pnas.0913022107
83. Yang Z, Rannala B (2014) Unguided species delimitation using DNA sequence data from multiple loci. Mol Biol Evol 31:3125–3135. https://doi.org/10.1093/molbev/msu279
84. Yasuda A (1913) Kinrui-zakki 19 (in Japanese). Bot Mag Tokyo 27:339–340

Tables

Tables 1 and 5 are available in the Supplementary Files section.

Figures

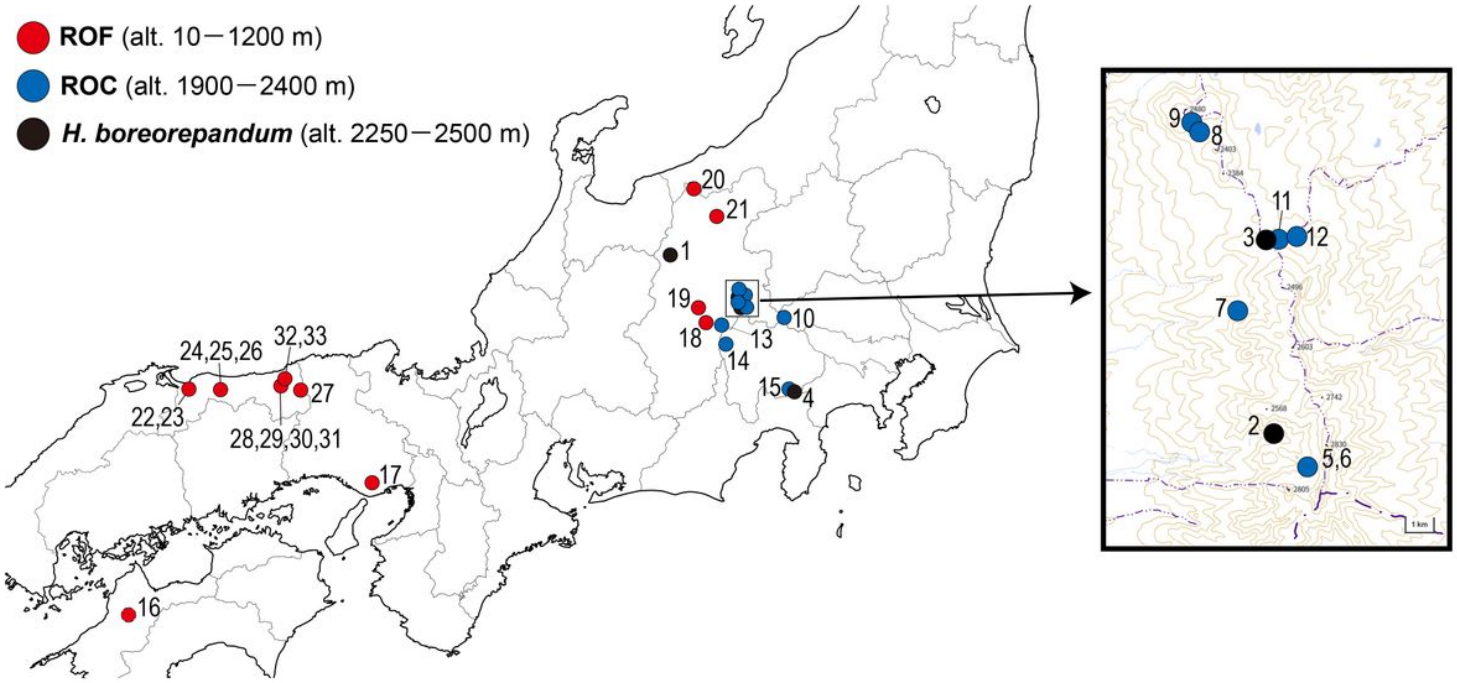

Figure 1

Collection sites in Japan. Number beside each site point is the site code in **Table 1**. The map was downloaded from the Geospatial Information Authority of Japan.

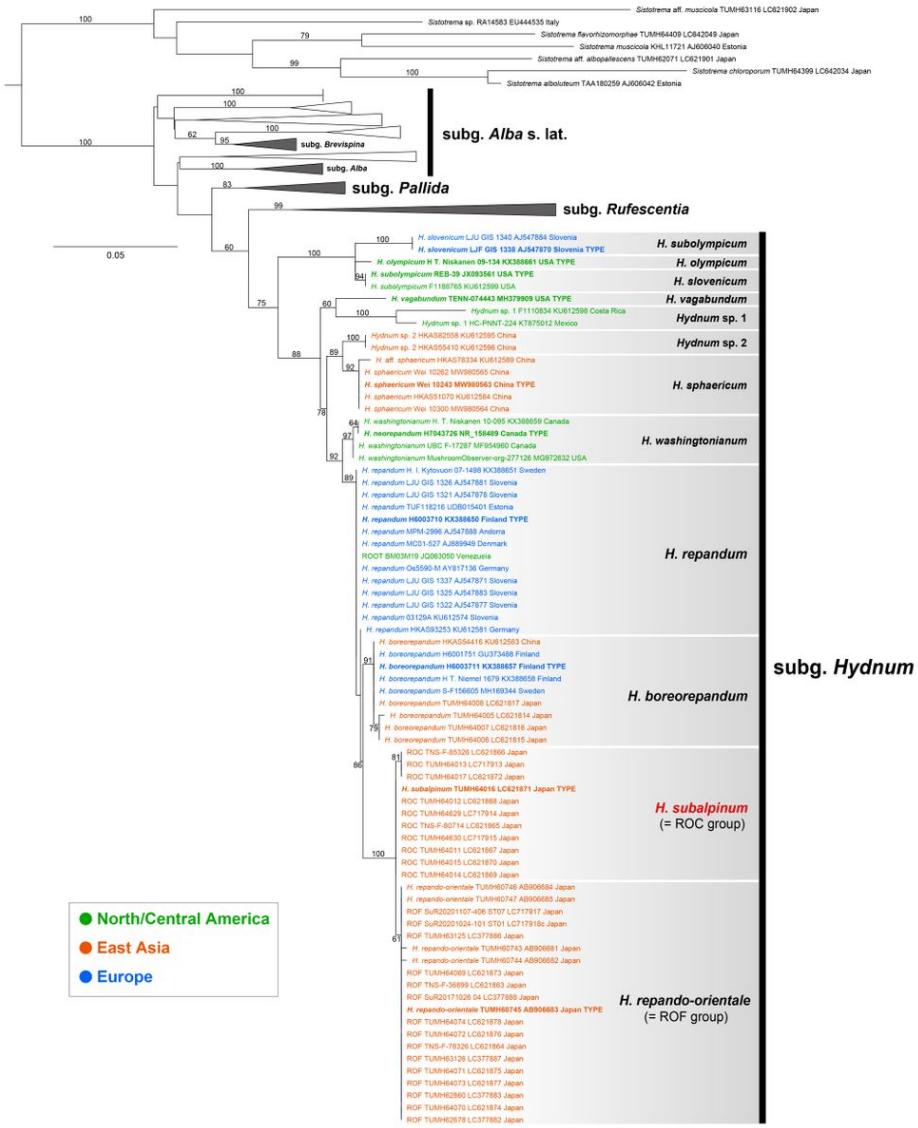

Figure 2

RAxML phylogram inferred from ITS sequences of Holarctic species of the genus *Hydnum*. Branches show statistical support in terms of maximum likelihood bootstrap (MLBS ≥ 60). In total, 175 sequences were included. *Hydnum* species of the subgenera *Alba* s. lat. (including *Alba* Niskanen & Liimat. and *Brevispina* T. Cao & H. S. Yuan), *Pallida* Niskanen & Liimat., and *Rufescentia* Niskanen & Liimat. were collapsed. Sequence color shows collection site: orange, East Asia; blue, Europe; green, Northern to Central America.

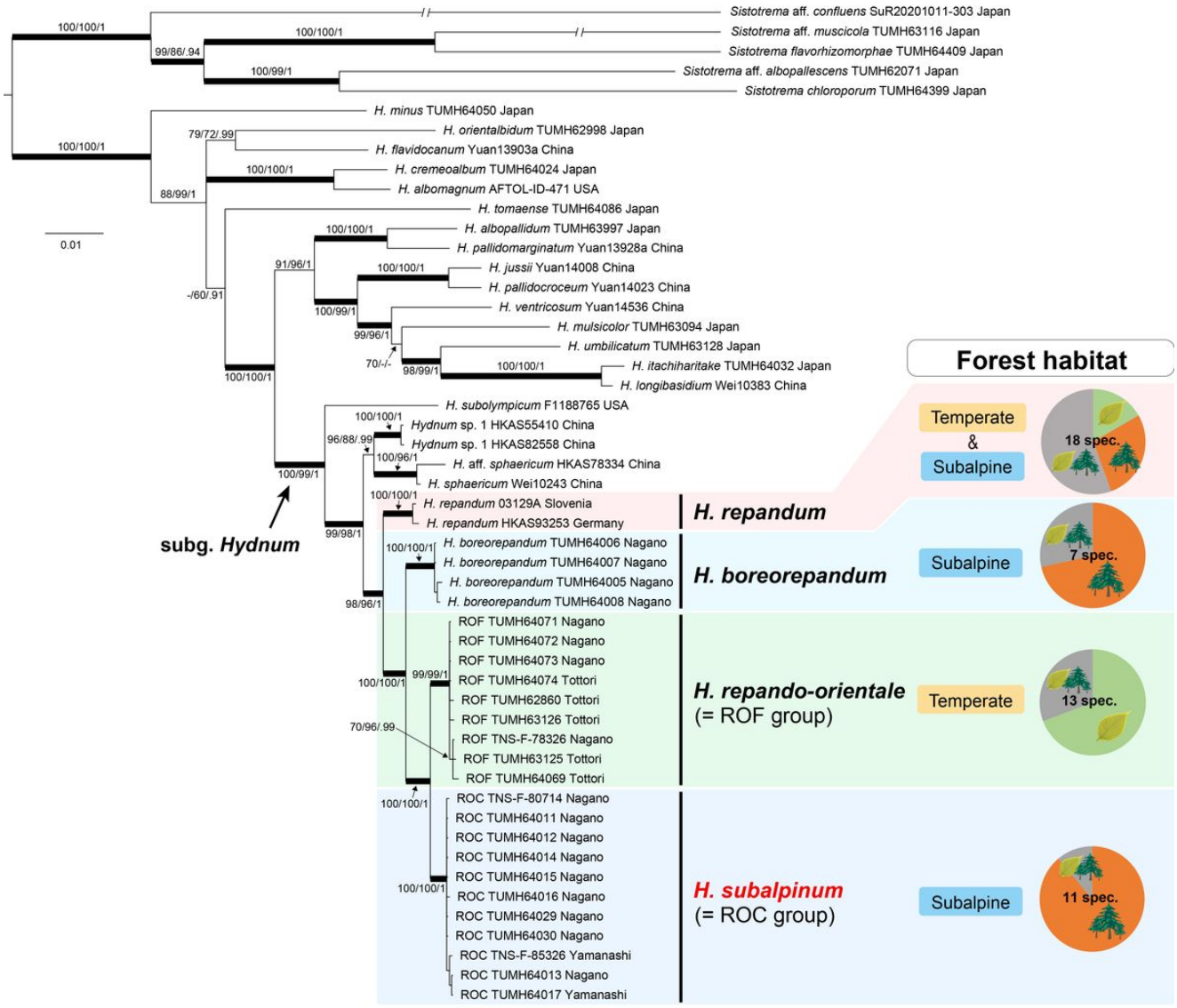

Figure 3

Bayesian phylogeny based on the concatenated dataset. Branches show statistical support in term of maximum likelihood bootstrap (MLBS ≥ 60), maximum-parsimony bootstrap (MPBS ≥ 60), and Bayesian inference posterior probability (BIP ≥ 0.90). Bold branches indicate strong support (MLBS ≥ 95, MPBS ≥ 95, BIP ≥ 0.95). Pie charts at left show forest habitats of the *H. repandum* and closely related species, referring to available collection information (broadleaf-dominated, coniferous-dominated, or mixed forests) and sequence data (Grebenc et al. 2009; Olariaga et al. 2012; Yanaga et al. 2015; Niskanen et al. 2018; Sugawara et al. 2022a).

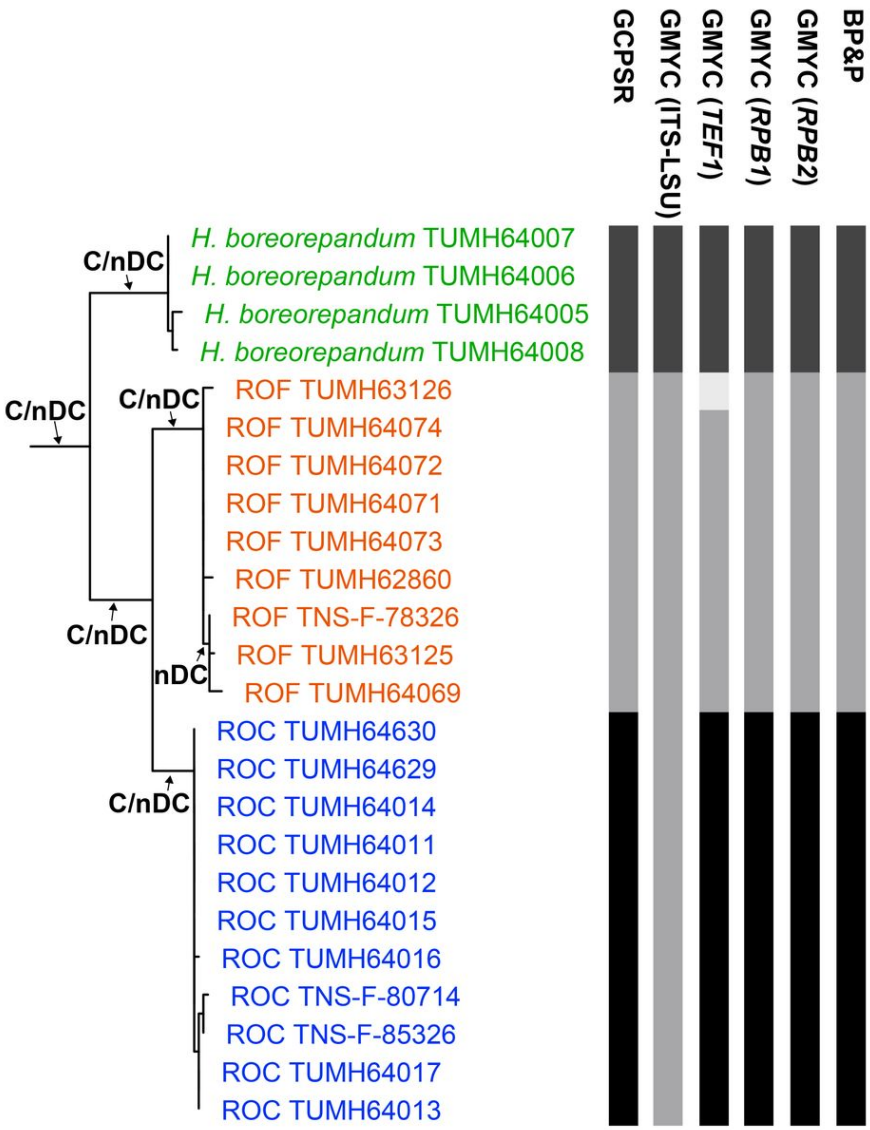

Figure 4

Species delimitations based on GCPSR, GMYC, and BP&P illustrated on the RAxML topology. Contrasting bars on left show best species boundaries. Branch shows phylogenetic concordance (C) and non-discordance (nDC)determined using the GCPSR approach.

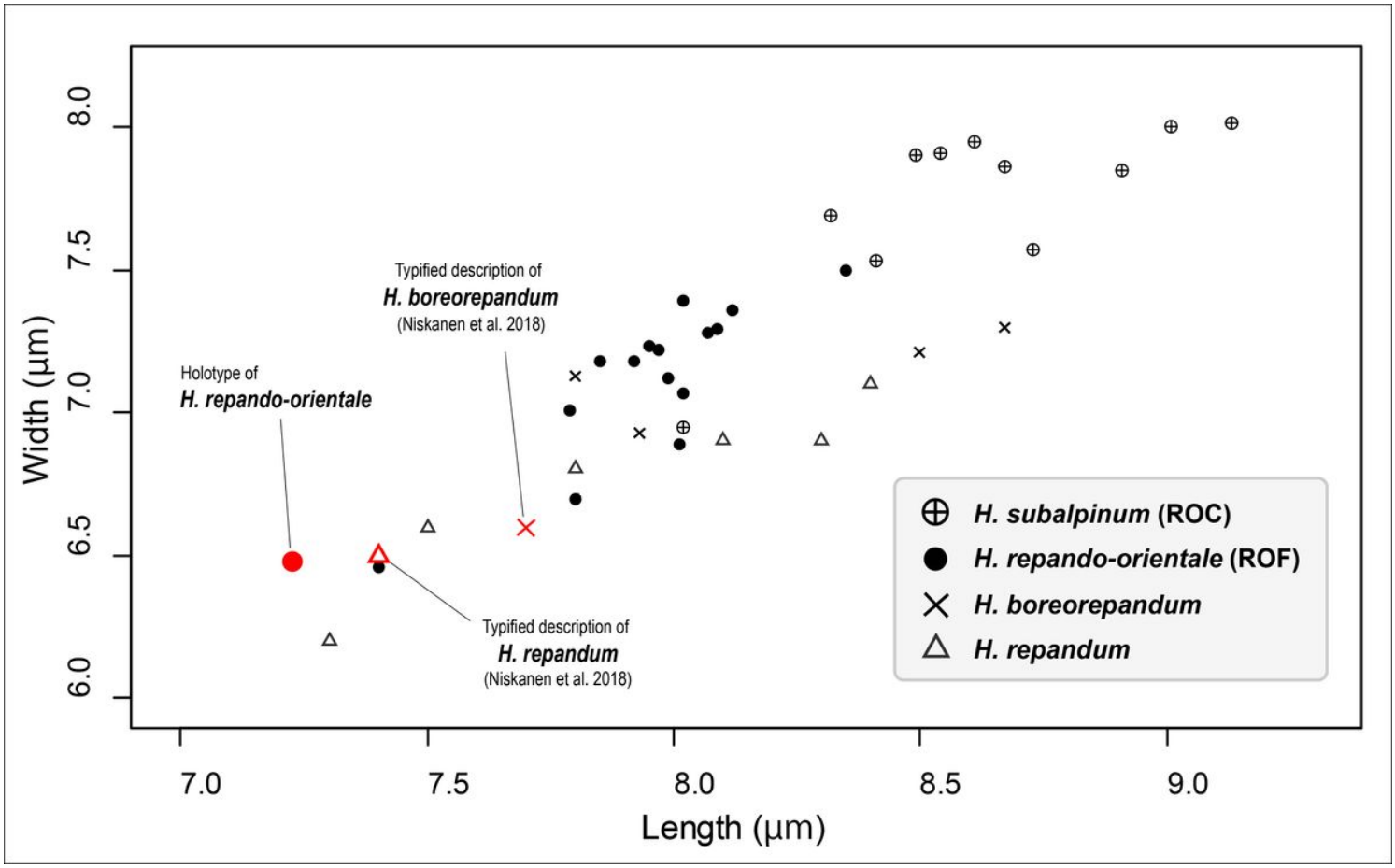

Figure 5

Basidiospore sizes of *Hydnum repando-orientale* and related species. Points are mean spore sizes of specimens of *H. subalpinum* (ROC; cross with circle), *H. repando-orientale* (ROF: black circle), *H. boreorepandum* (cross), or *H. repandum* (triangle). Also shown are previous measurements of *H. repandum* (Grebenc et al. 2009; Olariaga et al. 2012; Niskanen et al. 2018) and *H. boreorepandum* (Niskanen et al. 2018).

Figure 6

Macroscopic and microscopic features of *Hydnum subalpinum* (= ROC). **a–g** Macroscopic characters of Basidiomata (**a, b** TUMH 64016, holotype; **c** TUMH 640629; **d** TUMH 64014; **e** TUMH 64012; **f** TUMH 64630; **g** TUMH 64015). **h** Rhizomorphic hyphae underneath basidiomata (TUMH 64014). **i–k** Differential interference contrast micrographs of basidiospores (**i**), basidia (**j**), and hyphae of pileipellis in transverse sections (**k**), mounted with 3% KOH solution (TUMH 64016, holotype). **l** Monokaryotic culture ex-type incubated at 20 °C for 75 days (TUFC XXXXXX). Photographs: a, b, d, e, g–l, R. Sugawara; c, f, A. Koyama. *Bars*: d, e, l = 2 cm; i, j = 10 µm; k = 20 µm.

Supplementary Files

This is a list of supplementary files associated with this preprint. Click to download.

- Fig.S1.docx
- Fig.S2.docx
- Fig.S3.docx
- Fig.S4.docx
- Fig.S5.docx
- TableS1.docx
- TableS2.docx
- TableS3.docx

- TableS4.docx
- Table1.docx
- Table5.docx